Applicability of electride materials for hollow cathodes

IEPC-2019-A-604

Presented at the 36th International Electric Propulsion Conference
University of Vienna, Austria
September 15-20, 2019

Malina Reitemeyer*, Daniel Zschätzsch†, Kristof Holste‡, Limei Chen§ and Peter J. Klar¶
Institute of Experimental Physics I, Justus-Liebig-University Giessen
Heinrich-Buff-Ring 16, 35392 Giessen, Germany

Due to its low work function, the electride C12A7:e$^-$ emits electrons at significantly lower temperatures than state of the art neutralizer materials and is a promising insert candidate for a cold-cathode design. The material's electron density and, therefore, also the emission properties are influenced by the quality of the fabrication process and surface conditions. Understanding and influencing them subsequently, is part of our current research. In this work, the emission characteristics of C12A7:e$^-$ as a function of the applied temperature and voltage are presented. The work function was measured as 0.52 eV $\pm$ 0.03 eV. In addition, both an intrinsic electride sample and an oxidized sample are characterized by Raman spectroscopy. The Raman spectra reveal an electron density of the order of 10^{19}cm^{-3} to 10^{20}cm^{-3} for the electride and correspond to the spectrum of the ion conducting C12A7:O^{2-} in case of the oxidized sample.

Nomenclature

A_{G} = general Richardson constant
d = distance between anode and cathode
e = elementary charge
E = electric field
I = extracted current
I_{R} = zero field current
J = extracted current density
J_{R} = zero field current density
k_B = Boltzmann constant
S = emitting area of the sample
T = sample temperature
U = applied voltage
ϵ_0 = vacuum permittivity
Φ = work function

*Master student, malina.k.reitemeyer@physik.uni-giessen.de
†PhD cand., Daniel.Zschaetzsch@exp1.physik.uni-giessen.de
‡Senior Scientist, Kristof.Holste@exp1.physik.uni-giessen.de
§Senior Scientist, Limei.Chen@physik.uni-giessen.de
¶Director of Institute of Experimental Physics I, Head of EP-group, Peter.J.Klar@exp1.physik.uni-giessen.de

I. Introduction

ELECTRIC propulsion in space flight has grown in popularity over the last few years. Electric thrusters have a significantly higher specific impulse than chemical propulsion, which reduces the fuel consumption or increases the resulting Δv. Thus, they are very competitive in the low thrust regime (<1 N). These aspects are, on the one hand, advantageous for deep space missions, where a high velocity change is required. A recent prominent example is the BepiColombo mission with its QinetiQ T6 Kaufman ion engines[1]. On the other hand, the reduced working mass makes electric propulsion an interesting alternative to chemical propulsion systems for commercial missions, small satellites and satellite constellations, such as Starlink, which was launched recently[2]. Propulsion systems for these kind of missions have to provide low power consumption, high reliability, and a long lifetime.

Examples for electric propulsion systems are ion engines and Hall effect thrusters. These systems produce positively charged ions and accelerate them by an electric field. To prevent electric charge-up of the space craft, a neutralizer unit is needed, that emits electrons into the plume in order to compensate the positive ions leaving the spacecraft. In case of a Hall effect thruster, the electrons from the neutralizer are also needed to maintain the plasma inside the thruster by ionizing neutral gas atoms.

The most common neutralizer layout is the hollow cathode. A hollow cathode consists of a heat shield with a keeper and a cathode tube with a heater wired around it (see Fig. 1a). Within the cathode tube, an electron emitting insert is placed. State of the art neutralizers use insert materials like barium oxide inside a tungsten matrix (BaO-W) or lanthanum hexaboride (LaB6). These components all contribute to reliability, lifetime and power consumption of the overall system. According to Goebel and coworkers, the neutralizer is one of the main failure sources[3] of electric propulsion systems. Barium oxide and LaB6 are operated at about 1000 °C (BaO) and 1600 °C (LaB6), respectively[4], with a work function of 2.1 eV (BaO) and 2.7 eV (LaB6)[5]. These high temperatures reduce the efficiency of the thruster and put a high thermal stress on all constituents of the neutralizer, which often results in failures, typically induced by degradation or overheating of the insert or failure of the heater[6].

A promising insert material to avoid this problem is calcium aluminum based electride, also known as $[Ca_{12}Al_{14}O_{32}]^{4+}$:$4e^-$ or C12A7:e^-. Electrides are derived from an ionic compound, by replacing the anions bound in the lattice framework by electrons[7]. This results in a low work function of 0.6 eV for electron extraction[8]. The emission characteristics, in comparison with those of LaB6 and BaO, is shown in Fig. 1b. Of high interest is also the potential operation at room temperature, as shown by Ref. 9. This might allow a heater less design or at least a significantly lower heater temperature, which strongly reduces complexity and increases reliability and lifetime of the neutralizer. As a potential neutralizer insert candidate, the electride material was first investigated at Colorado State University[10] and also at TU Dresden[11]. The results are very promising with discharge currents up to 2.8 A[12].

However, also the use of C12A7:e^- raises some challenges to be mastered by the design. On the one hand, C12A7 has one order of magnitude lower thermal conductivity than LaB6[13–14], what may easily lead to overheating of the cathode. Furthermore, the long term stability under ambient atmosphere has to be further investigated. In addition, the emission characteristics, i.e. the resulting emission current, depend upon the electron density within the material, which is influenced by the fabrication process. Due to a reduction, the electron concentration within the electride can be tailored starting from ion conducting mayenite. Understanding and steering this process is important to make full use of the material's potential.

In this paper, the characterization of commercially available C12A7:e^--samples is presented with a particular focus on the material's work function. In section II the material C12A7:e^- is described in detail. The experimental setup and the samples used are described in III and characterised by Raman spectroscopy in section IV. Finally, the emission characteristics of an C12A7:e^--sample in dependence on the applied voltage and temperature are discussed in section V. Section VI concludes the paper.

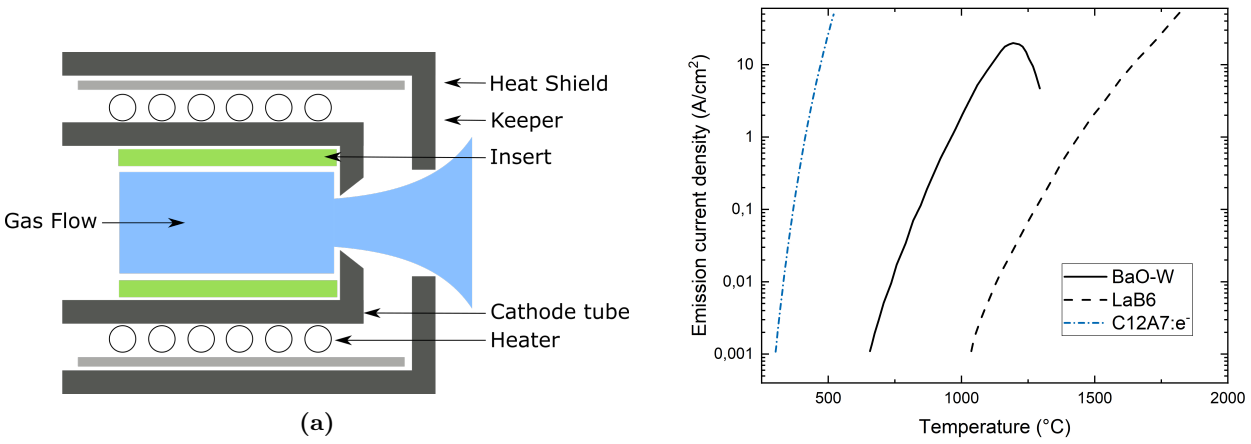

(a) (b)

Figure 1: a) Schematic image of a typical neutralizer, inspired by Ref. 15 b) Emission currents of various neutralizer insert materials in dependency of the insert temperature, own chart, data taken from Ref. 16

II. Material Description

Electrides are materials where electrons occupy lattice sites in crystals, normally populated by anions. At these sites, they are neither completely localized, nor free[17]. In 1988, when Lacerda and coworkers reported first on the high ionic conductivity[18] of calcium aluminate mayenite $Ca_{12}Al_{14}O_{33}$, one critical factor in examining electride material was the stability at room temperature and ambient atmosphere (including oxygen). However, in 2003 Matsuishi et al.[19] presented the first air- and room temperature stable inorganic electride. As primary material they used the calcium aluminate Mayenite, or in systematic nomenclature $12CaO\text{-}7Al_2O_3$ [20]. Hereafter, it will be referred to as C12A7.

C12A7 is ordered in a unique cage structure (see Fig. 2a left), where AlO_4 tetrahedra form in conjunction with seven calcium ions twelve cages per unit cell. Due to the positively charged lattice framework, the cages can contain four negative elementary charges per unit cell. Various anions, like O^{2-} or F^- can be incorporated in these cages to tailor the material's chemical and physical properties[21].

To synthesize an electride from this material, the (oxygen) anions have to be removed by reduction and be replaced by four electrons. This can either be archived by a melt-solidification or a glass-ceramic process. Further details are given in Ref. 8. The result is C12A7 with four electrons per unit cell: $[Ca_{24}Al_{28}O_{64}]^{4+}:4e^-$. Given the length of a unit cell of 1.199 nm [19], the theoretical maximum value for the electron density is $2.33 \cdot 10^{21}\,cm^{-3}$ [8].

The values determined for the work function are mostly in the range of 0.6 eV [8,9,11]. Due to the low work function, electrides are promising candidates for hollow cathode inserts.

III. Experimental setup

For the electron extraction a simple anode-cathode design was developed (see Fig. 2b): With an applied electric field, electrons are extracted from the sample at different temperatures. The cathode is biased negative with respect to ground potential. This negative bias can be varied between 0 V and 2 kV during the data collection to examine the impact of the electric field on electron emission. The distance between the anode and the cathode was 2 mm. Graphite was used as cathode material as it can withstand the high temperatures up to 500 °C used in the setup without evaporation under vacuum conditions.

For the first setup design, the resistance between the anode and the cathode decreased down to 150 kΩ

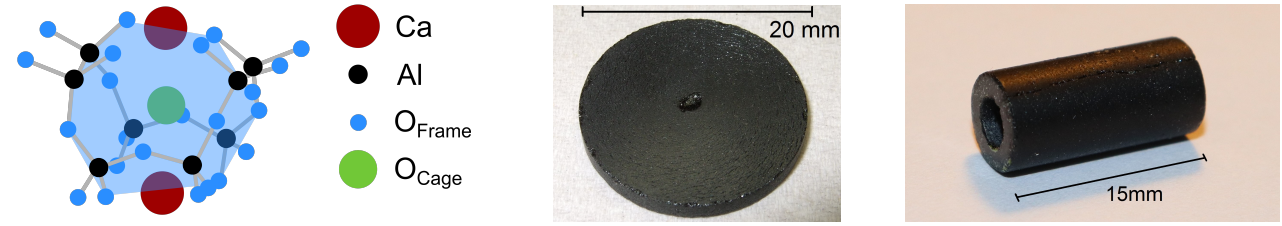

(a)

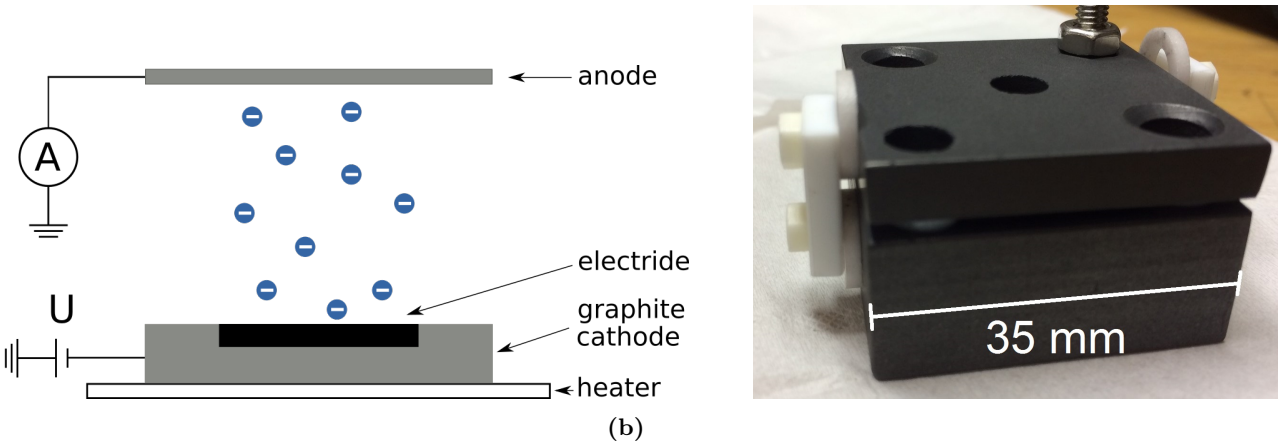

(b)

Figure 2: a) On the left: Electride cage structure. The cage is formed by aluminum tetrahedra in conjunction with calcium. In this lattice framework an O^{2-} anion is bound. Inspired by Ref. 22; Center and right: Electride samples provided by ATD b) Experimental setup used for extraction with a schematic view without insulators between cathode and anode on the left and a photograph of the setup outside of the vacuum chamber without cables and heater on the right

at 700 °C heater temperature, which resulted in high leak currents up to 9 μA/cm^2 at 540 °C heater temperature. Since this decrease of resistance can be counteracted by an increase of the resistor length to cross section ratio, a c-shaped construction was designed to hold the anode, which can be seen in Fig. 2b. The sample is placed within a recess in the graphite cathode, where it is heated by the thermal contact to the cathode.

As a heater, an UHV heater stage by *tectra* was used. It contains graphite as electrically conducting material, coated with pyrolytic boron nitrite (PBN). The heater plate can reach temperatures up to 1500 °C, which covers the whole temperature range needed for studying the electronic emission of C12A7:e$^-$. In the beginning, the proportional–integral–derivative (PID) heater controller, provided by *Rievtech* was used. However, currents, induced by the alternating heater current, were detected at the cathode, so a DC-power-supply is used instead.

The temperature was measured through an IR-transmitting window on top of the setup with a thermal imaging camera supplied by *micro-epsilon*. This camera is sensitive up to 900 °C, which matches well the temperature range needed for C12A7:e$^-$ emission measurements. For measurements at higher temperatures, for example to conduct comparative measurements with LaB6, a pyrometer may be used.

All tests were conducted in ultra high vacuum at pressures below 10^{-7} mbar. Since C12A7:e$^-$ reacts very sensitively upon oxygen contamination, a mass spectrometer was used to determine the oxygen partial pressure, which is about $5 \cdot 10^{-11}$ mbar in the test chamber.

The samples used for the tests described in this paper were provided by *Advanced Thermal Devices* (ATD). To measure the material's work function, 20 mm diameter disks were used. For later neutralizer tests, hollow

cylinder inserts are available. Pictures of the electride samples are shown in Fig. 2a. For a better electrical and thermal contact between the cathode and the sample, the disk samples were coated with platinum on the bottom side and the circumference (not shown in the pictures).

IV. Raman spectroscopy

The resulting emission current is linked to the material's electron density. This density also influences the Raman spectrum of a sample. Kim et al.[23] recorded Raman spectra for C12A7 materials with different electron and oxygen densities with 457 nm laser exitation. They showed, that some Raman signals are proportional to the material's electron and oxygen densities: 186 cm^{-1} is only visible at high electron densities and increases with electron density. The same holds for the intensity ratio of the 430 cm^{-1} band relative to the 780 cm^{-1} band. For the 560 cm^{-1} band a decrease occurs with increasing electron density (see Fig. 3a).

To characterize our sample and determine the electron density N_e, a Raman spectrum at 488 nm wavelength was taken for an electride sample. The spectrum is given in Fig. 3b (blue line). It shows to minor bands around 160 cm^{-1} and a broad maximum around 350 cm^{-1}. Two additional bands can be found around 560 cm^{-1}. Also, strong signals were recorded above 750 cm^{-1}. Since the bands at 186 cm^{-1} and 430 cm^{-1} are not very dominant in the spectrum, the electron density within the material is presumably not very high. In comparision with Fig. 3a, the electron density can be estimated to lie between $10^{19}\,\mathrm{cm}^{-3}$ and $10^{20}\,\mathrm{cm}^{-3}$

One of our samples was exposed at 1000 °C to an Ar-H_2 atmosphere for 24 hours. After the treatment, the sample lost its black color and has now a more pile-transparent appearance (see lower insert in Fig. 3b). This may be traced back to residual oxygen within the gas atmosphere, which oxidized the sample. To verify this assumption, a Raman spectrum was measured. The spectrum can be found in Fig. 3b (yellow line). Strong bands can be seen at 181 cm^{-1}, 309 cm^{-1}, 520 cm^{-1} and 771 cm^{-1} . Compared to the spectra in Fig. 3a, this spectrum shows good agreement with the spectrum of a C12A7:O^{2-}-crystal. The measured signals from 150 cm^{-1} to 350 cm^{-1}, therefore, correspond to cage vibrations within the crystal. In the absence of a high electron concentration, no sharp band at 186 cm^{-1} could be measured. Same can be said for the 430 cm^{-1} band, where no significant peak can be seen. However, a strong peak is visible at 520 cm^{-1}, which is a sign for a high oxygen concentration. This confirms the hypothesis, that the sample is not longer an electride but is oxidized to the ionic ceramic mayenite C12A7:O^{2-}. Normally, oxidized C12A7:O^{2-} ceramic is rather clear transparent than colored, but in Ref. 24 an orange tint was also reported. In that case, iridium ions from the fabrication crucible were causing the contamination.

V. Results

A. Work-Function

The work function Φ is a crucial parameter for the electron emission. The first expression to determine the work function from the temperature dependent emission current was given by Richardson

$$I_\mathrm{R} = S A_\mathrm{G} T^2 \exp\left(-\frac{\Phi}{k_B T}\right) \tag{1}$$

where I_R is the emitted current, S the surface area, T the sample temperature and A_G a constant. Within the setup, as described in section III, a high negative voltage is used for electron extraction. Therefore, the work function given above has to be corrected by a Schottky-factor $\Delta\Phi_\mathrm{S}$

$$\Delta\Phi_\mathrm{S} = \sqrt{\frac{e^3 E}{4\pi\epsilon_0}} \tag{2}$$

with the applied electric field $E = d \cdot U_\mathrm{acc}$. Considering this correction, the following expression for the current density $J = I/S$

$$J = A_\mathrm{G} T^2 \exp\left(-\frac{\Phi - \Delta\Phi}{k_B T}\right) \tag{3}$$

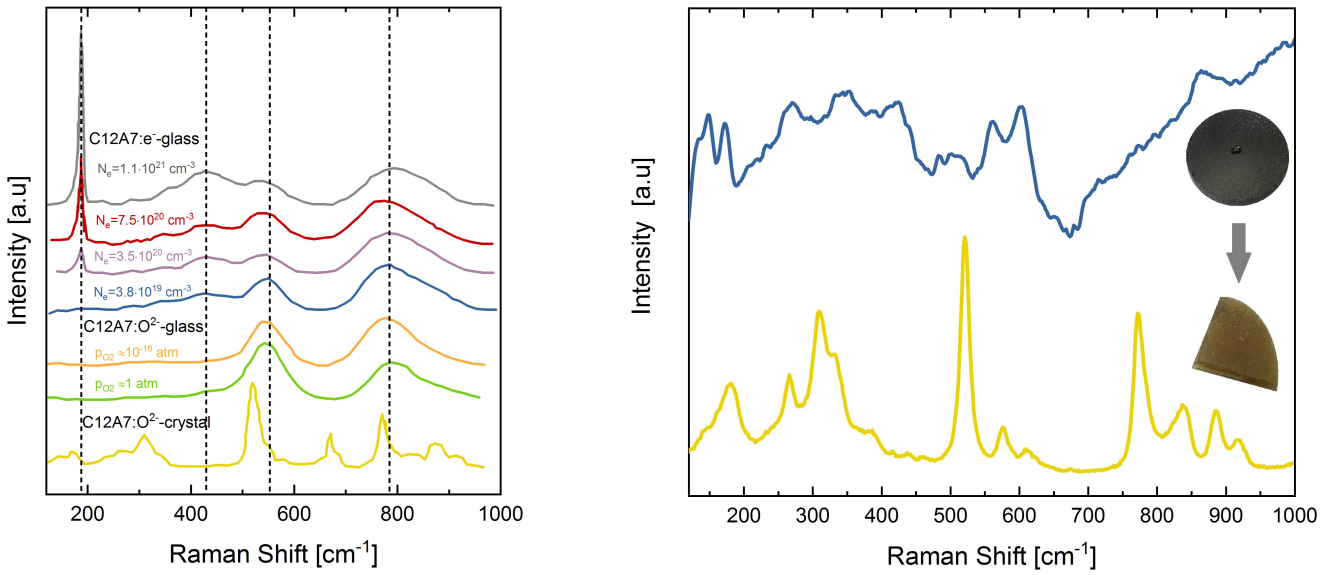

Figure 3: Raman spectra of C12A7 samples: a) Raman spectra of C12A7 as measured in Ref. 23: The spectra show resonance lines for various electron and oxygen densities of C12A7 b) Raman spectra of an electride sample (blue line) and of an oxidized sample (yellow line), which was exposed to an Ar-H_2 atmosphere. Pictures of the samples are shown in the insert

$$= A_{\mathrm{G}} T^2 \exp\left(-\frac{\Phi}{k_B T}\right) \cdot \exp\left(\frac{e}{k_B T}\sqrt{\frac{edU}{4\pi\epsilon_0}}\right) \tag{4}$$

$$= J_{\mathrm{R}} \exp\left(\frac{e}{k_B T}\sqrt{\frac{edU}{4\pi\epsilon_0}}\right) \tag{5}$$

can be derived. The work function Φ can therefore be determined in two steps. First, a so called Schottky-Plot ($\ln(J)$ as a function of $\sqrt{U}$) is used to extract J_R, the scope of the linear fit, in dependence of the sample temperature. Second, $\ln(J_R/T^2)$ is plotted against $1000/T$, the so called Richardson-Plot. The work function is given by the slope m of the linear fit to this plot

$$\Phi = -m \cdot 1000\, k_B \ . \tag{6}$$

B. C12A7 measurements

The current extracted from the electride as a function of the applied voltage is shown for various temperatures in Fig. 4a. At 500 V and 500 °C sample temperature an emission current of 0.08 μA/cm^2 is obtained. As it can easily be seen, the emission current strongly varies with the applied voltage and sample temperature (see for this also Eq. 5).

In total six different sample temperatures were measured over a wide range of extraction voltages (typically 20 V to 1800 V). The corresponding Schottky-plots can be found in Fig. 4b. For voltages from 200 V to 1000 V, the curves show a linear behavior. From this graph, the y-intercepts of the linear regions can be extracted to determine J_R. The J_R-values for different temperatures are plotted in Fig. 4b (lower graph). The slope of the linear fit is $m = -6.03$ K, which results in a work function of 0.52 eV with an statistical error of 0.03 eV. This result is in very good coherence with Refs 8, 9, and 11.

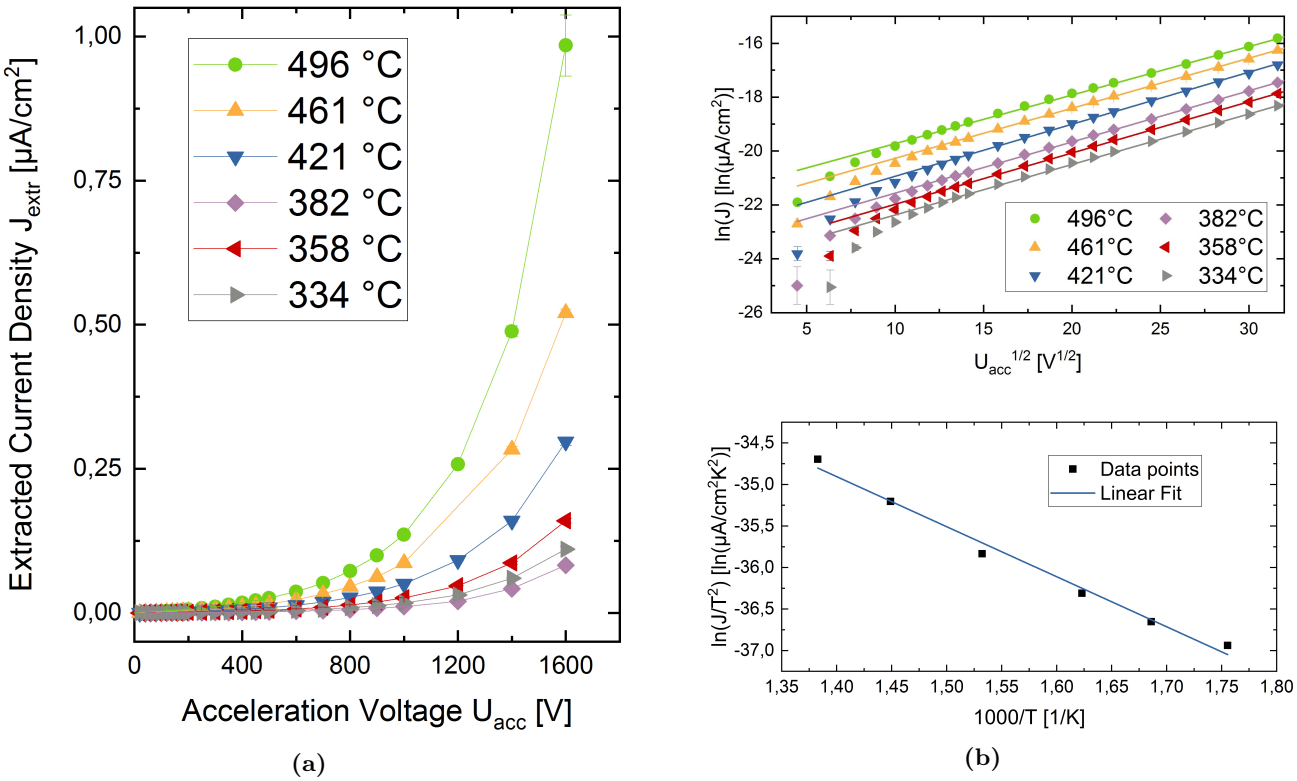

Figure 4: a) Electron emission current as a function of the applied voltage for different sample temperatures b) Plots to extract the work function from the given current emission. The top graph is a Schottky-Plot for emission at different extraction voltages and temperatures. From the lower plot, a Richardson-Plot, the work function can be extracted from the slope

VI. Conclusion

We obtained a value for the work function of 0.52 eV ± 0.03 eV for C12A7:e$^-$ of a low electron concentration between 10^{19}cm^{-3} and 10^{20}cm^{-3} and corresponding currents of 1 μA/cm^2. In addition, one sample was successfully oxidized and this way the mayenite ceramic character of the basis material confirmed. With Raman spectroscopy, the change in the C12A7-cages could be verified. Another aspect, which is currently of major interest, are emission characteristics under different gas atmospheres with a particular focus on the long term current stability. Measurements presented here, provide important knowledge to extract construction parameters for future hollow cathode devices based on C12A7:e$^-$.

Acknowledgments

This work has been supported by the German Aerospace Center under contract 50RK1948 in the framework of the ECHO project. D. Zschätzsch thanks *ArianeGroup* for the provision of his PhD studentship.

References

[1] Hutchins, M., Simpson, H., Palencia Jiménez, J. "QinetiQ's T6 and T5 Ion Thruster Electric Propulsion System Architectures and Performances", *International Electric Propulsion Conference IEPC*, CP91524, Vol. 34, Kobe, 2015

[2] Foust, Jeff "SpaceX's space-Internet woes: Despite technical glitches, the company plans to launch the first of nearly 12,000 satellites in 2019", *IEEE Spectr.*, Vol. 56, No. 1, 2019, pp. 50–51

[3] Goebel, D. M., Polk, J. E., Sandler, I., Mikellides, I. G.; Brophy, J. R. "Evaluation of 25-cm XIPS©

Thruster Life for Deep Space Mission Applications", *International Electric Propulsion Conference IEPC*, CP152, Vol. 31, Ann Arbor, Michigan, 2009

[4] Rand, L. P., Williams, J.D. "Instant Start Electride Hallow Cathode" *International Electric Propulsion Conference IEPC*, CP305, Vol. 33, Washington, DC, 2013

[5] Goebel, D. M.; Watkins, R. M.; Jameson, K. K. "LaB6 Hollow Cathodes for Ion and Hall Thrusters" *J. Propul. Power*, Vol. 23, No. 3, 2007, pp. 552–558

[6] D.Goebel, D. M., Katz, I., *Fundamentals of electric propulsion. Ion and Hall thrusters*, JPL space science and technology series, 1st ed., Wiley, Hoboken, N.J, 2008, Chap. 6

[7] Kim, S.W., Miyakawa, M., Hayashi, K., Sakai, T.,Hirano, M. , Hosono, H. "Simple and efficient fabrication of room temperature stable electride: melt-solidification and glass ceramics" *J. Am. Chem. Soc.*, Vol. 127, No. 5, 2005, pp. 1370–1371

[8] Kim, S.W., Toda, Y., Hayashi, K., Hirano, M., Hosono, H. "Synthesis of a Room Temperature Stable 12CaO·7Al 2 O 3 Electride from the Melt and Its Application as an Electron Field Emitter" *Chem. Mater.*, Vol. 18, No. 7, 2006, pp. 1938–1944

[9] Toda, Y., Matsuishi, S., Hayashi, K., Ueda, K., Kamiya, T., Hirano, M., Hosono, H. "Field Emission of Electron Anions Clathrated in Subnanometer-Sized Cages in [Ca24Al28O64]4+(4e-)" *Adv. Mater.*, Vol. 16, No. 8, 2004, pp. 685-689

[10] Rand, L., Williams, J., Hoyt, R. "Hollow Cathode with Electride Insert" *47th AIAA/ASME/SAE/ASEE Joint Propulsion Conference & Exhibit*, CP5992, AIAA, Washington, 2011

[11] Bock, D., Drobny, C., Laufer, P., Kössling, M., Tajmar, M. "Development and Testing of Electric Propulsion Systems at TU Dresden" *Propulsion and Energy Forum. AIAA/SAE/ASEE Joint Propulsion Conference*, CP4848, Vol. 52, Salt Lake City, UT, 2016

[12] Rand, L., "A calcium aluminate electride hollow cathode" Ph.D. Dissertation, Colorado State University, Colorado, 2014

[13] Kim, S. W., Tarumi, R., Iwasaki, H., Ohta, H., Hirano, M., Hosono, H. " Thermal conductivity and Seebeck coefficient of 12CaO-7Al2O3 electride with a cage structure", *Phys. Rev. B*, Vol. 80, No. 7, 2009, p. 075201

[14] Popov, P. A., Novikov, V. V., Sidorov, A. A., Maksimenko, E. V. "Thermal conductivity of LaB6 and SmB6 in the range 6–300 K", *Inorg. Mater.*, Vol. 43, No. 11, 2007, pp. 1187–1191

[15] Wordingham, C. J., Taunay, P., Choueiri, E. "A Critical Review of Orificed Hollow Cathode Modeling: 0D Models" *53rd AIAA/SAE/ASEE Joint Propulsion Conference*, AIAA, Washington, 2017, S. 611.

[16] Lev, D. R., Mikellides, I. G., Pedrini, D., Goebel, D. M., Jorns, B. A.; McDonald, M. S. "Recent progress in research and development of hollow cathodes for electric propulsion" *Rev. Mod. Plasma Phys.*, Vol. 3,Is. 1, 2019, p.1560

[17] Dye, J. "Chemistry. Electrons as anions" *Science*, Vol. 301, No. 5633, 2009, pp. 607–608

[18] Lacerda, M., Irvine, J. T. S., Glasser, F. P., West, A. R. "High oxide ion conductivity in Ca 12 Al 14 O 33", *Nature*, Vol. 332, No. 6164, 1988, pp. 525–526

[19] Matsuishi, S., Toda, Y., Miyakawa, M., Hayashi, K., Kamiya, T., Hirano, M., et al. "High-density electron anions in a nanoporous single crystal. $[Ca_{24}Al_{28}O_{64}]^{4+}(4e^-)$" *Science*, Vol. 301, No. 5633, 2003, pp. 626–629

[20] Boysen, H., Lerch, M., Stys, A., Senyshyn, A. "Structure and oxygen mobility in mayenite (Ca12Al14O33): a high-temperature neutron powder diffraction study" *Acta cryst. B*, Vol. 63, No. 5 2007, pp. 675–682

[21] Volodin, A. M., Zaikovskii, V. I., Kenzhin, R. M., Bedilo, A. F., Mishakov, I. V., Vedyagin, A. A. "Synthesis of nanocrystalline calcium aluminate C12A7 under carbon nanoreactor conditions" *Mater. Lett.*, Vol. 189, 2017, pp. 210–212

[22] Lee, D.K., Kogel, L., Ebbinghaus. S.G., Valov, I., Wiemhoefer, H.D., Lerch, M., Janek, J., "Defect chemistry of the cage compound, Ca12Al14O33d: understanding the route from a solid electrolyte to a semiconductor and electride" *Phys. Chem. Chem. Phys.*, Vol. 11, No. 17, 2009, p. 3010

[23] Kim, S.W., Shimoyama, T., Hosono, H., "Solvated electrons in high-temperature melts and glasses of the room-temperature stable electride $[Ca_{24}Al_{28}O_{64}]^{4+}\cdot 4e^-$" *Science*, Vol. 333, No. 6038, 2011, pp. 71–74

[24] Kim, S.W., Matsuishi, S., Nomura, T., Kubota, Y., Takata, M., Hayashi, K. et al. "Metallic state in a lime-alumina compound with nanoporous structure" *Nano letters*, Vol. 7, No. 5, 2007, pp. 1138–1143